This document was prepared by the DUNE collaboration using the resources of the Fermi National Accelerator Laboratory (Fermilab), a U.S. Department of Energy, Office of Science, HEP User Facility. Fermilab is managed by Fermi Research Alliance, LLC (FRA), acting under Contract No. DE-AC02-07CH11359.

The DUNE collaboration also acknowledges the international, national, and regional funding agencies supporting the institutions who have contributed to completing this Technical Design Report.

Authors

B. Abi,[129] R. Acciarri,[56] Mario A. Acero,[8] G. Adamov,[59] D. Adams,[15] M. Adinolfi,[14] Z. Ahmad,[163] J. Ahmed,[166] T. Alion,[153] S. Alonso Monsalve,[18] C. Alt,[49] J. Anderson,[4] C. Andreopoulos,[109] M. P. Andrews,[56] F. Andrianala,[2] S. Andringa,[103] A. Ankowski,[143] J. Anthony,[28] M. Antonova,[72] S. Antusch,[9] A. Aranda Fernandez,[36] A. Ariga,[10] L. O. Arnold,[39] M. A. Arroyave,[48] J. Asaadi,[157] A. Aurisano,[34] V. Aushev,[101] D. Autiero,[81] F. Azfar,[129] H. Back,[130] J. J. Back,[166] C. Backhouse,[161] P. Baesso,[14] L. Bagby,[56] R. Bajou,[1] S. Balasubramanian,[170] P. Baldi,[23] B. Bambah,[70] F. Barao,[103, 105] G. Barenboim,[72] G. J. Barker,[166] W. Barkhouse,[123] C. Barnes,[116] G. Barr,[129] J. Barranco Monarca,[64] N. Barros,[103, 106] J. L. Barrow,[155, 56] A. Bashyal,[128] V. Basque,[114] F. Bay,[122] J. L. Bazo Alba,[137] J. F. Beacom,[127] E. Bechetoille,[81] B. Behera,[38] L. Bellantoni,[56] G. Bellettini,[135] V. Bellini,[74] O. Beltramello,[18] D. Belver,[19] N. Benekos,[18] F. Bento Neves,[104] J. Berger,[136] S. Berkman,[56] P. Bernardini,[144] R. M. Berner,[10] H. Berns,[22] S. Bertolucci,[73] M. Betancourt,[56] Y. Bezawada,[22] M. Bhattacharjee,[86] B. Bhuyan,[86] S. Biagi,[152] J. Bian,[23] M. Biassoni,[76] K. Biery,[56] B. Bilki,[11] M. Bishai,[15] A. Bitadze,[114] A. Blake,[107] B. Blanco Siffert,[55] F. D. M. Blaszczyk,[56] G. C. Blazey,[124] E. Blucher,[32] J. Boissevain,[110] S. Bolognesi,[17] T. Bolton,[98] M. Bonesini,[76] M. Bongrand,[102] F. Bonini,[15] A. Booth,[153] C. Booth,[146] S. Bordoni,[18] A. Borkum,[153] T. Boschi,[47] N. Bostan,[90] P. Bour,[41] S. B. Boyd,[166] D. Boyden,[124] J. Bracinik,[12] D. Braga,[56] D. Brailsford,[107] A. Brandt,[157] J. Bremer,[18] C. Brew,[142] E. Brianne,[114] S. J. Brice,[56] C. Brizzolari,[76] C. Bromberg,[117] G. Brooijmans,[39] J. Brooke,[14] A. Bross,[56] G. Brunetti,[131] N. Buchanan,[38] H. Budd,[140] D. Caiulo,[81] P. Calafiura,[108] J. Calcutt,[117] M. Calin,[16] S. Calvez,[38] E. Calvo,[19] L. Camilleri,[39] A. Caminata,[75] M. Campanelli,[161] D. Caratelli,[56] G. Carini,[15] B. Carlus,[81] P. Carniti,[76] I. Caro Terrazas,[38] H. Carranza,[157] A. Castillo,[145] C. Castromonte,[89] C. Cattadori,[76] F. Cavalier,[102] F. Cavanna,[56] S. Centro,[131] G. Cerati,[56] A. Cervelli,[73] A. Cervera Villanueva,[72] M. Chalifour,[18] C. Chang,[25] E. Chardonnet,[1] A. Chatterjee,[136] S. Chattopadhyay,[163] J. Chaves,[132] H. Chen,[15] M. Chen,[23] Y. Chen,[10] D. Cherdack,[69] C. Chi,[39] S. Childress,[56] A. Chiriacescu,[16] K. Cho,[97] S. Choubey,[66] A. Christensen,[38] D. Christian,[56] G. Christodoulou,[18] E. Church,[130] P. Clarke,[50] T. E. Coan,[150] A. G. Cocco,[78] J. A. B. Coelho,[102] E. Conley,[46] J. M. Conrad,[115] M. Convery,[143] L. Corwin,[147] P. Cotte,[17] L. Cremaldi,[119] L. Cremonesi,[161] J. I. Crespo-Anadón,[39] E. Cristaldo,[6] R. Cross,[107] C. Cuesta,[19] Y. Cui,[25] D. Cussans,[14] M. Dabrowski,[15] H. da Motta,[30] L. Da Silva Peres,[55] Q. David,[81] G. S. Davies,[119] S. Davini,[75] J. Dawson,[1] K. De,[157] R. M. De Almeida,[58] P. Debbins,[90] I. De Bonis,[20] M. P. Decowski,[122] A. de Gouvêa,[125] P. C. De Holanda,[29] I. L. De Icaza Astiz,[153] A. Deisting,[85] P. De Jong,[122] A. Delbart,[17] D. Delepine,[64] M. Delgado,[3] A. Dell'Acqua,[18] P. De Lurgio,[4] J. R. T. de Mello Neto,[55] D. M. DeMuth,[162] S. Dennis,[109] C. Densham,[142] G. Deptuch,[56] A. De Roeck,[18] V. De Romeri,[72] J. J. De Vries,[28] R. Dharmapalan,[68] F. Diaz,[137] J. S. Díaz,[88] S. Di Domizio,[75] L. Di Giulio,[18] P. Ding,[56] L. Di Noto,[75] C. Distefano,[152] R. Diurba,[160] M. Diwan,[15] Z. Djurcic,[4] N. Dokania,[151] M. J. Dolinski,[45] L. Domine,[143] D. Douglas,[117] F. Drielsma,[143] D. Duchesneau,[20] K. Duffy,[56] P. Dunne,[85] T. Durkin,[142] H. Duyang,[149] O. Dvornikov,[68] D. A. Dwyer,[108] A. S. Dyshkant,[124] M. Eads,[124] D. Edmunds,[117] J. Eisch,[91] S. Emery,[17] A. Ereditato,[10] C. O. Escobar,[56] L. Escudero Sanchez,[28] J. J. Evans,[114] K. Ewart,[88] A. C. Ezeribe,[146] K. Fahey,[56] A. Falcone,[76] C. Farnese,[131] Y. Farzan,[82] J. Felix,[64] E. Fernandez-Martinez,[113] P. Fernandez Menendez,[72] F. Ferraro,[75] L. Fields,[56] A. Filkins,[168] F. Filthaut,[122] R. S. Fitzpatrick,[116] W. Flanagan,[43] B. Fleming,[170] R. Flight,[140] J. Fowler,[46] W. Fox,[88] J. Franc,[41] K. Francis,[124] D. Franco,[170] J. Freeman,[56] J. Freestone,[114] J. Fried,[15] A. Friedland,[143] S. Fuess,[56] I. Furic,[57] A. P. Furmanski,[160] A. Gago,[137] H. Gallagher,[159] A. Gallego-Ros,[19] N. Gallice,[77, 76] V. Galymov,[81] E. Gamberini,[18] T. Gamble,[146] R. Gandhi,[66] R. Gandrajula,[117] S. Gao,[15] D. Garcia-Gamez,[62] M. Á. García-Peris,[72] S. Gardiner,[56] D. Gastler,[13] G. Ge,[39] B. Gelli,[29] A. Gendotti,[49] S. Gent,[148] Z. Ghorbani-Moghaddam,[75] D. Gibin,[131] I. Gil-Botella,[19] C. Girerd,[81] A. K. Giri,[87] D. Gnani,[108] O. Gogota,[101] M. Gold,[120] S. Gollapinni,[110] K. Gollwitzer,[56] R. A. Gomes,[52] L. V. Gomez Bermeo,[145] L. S. Gomez Fajardo,[145] F. Gonnella,[12] J. A. Gonzalez-Cuevas,[6] M. C. Goodman,[4] O. Goodwin,[114] S. Goswami,[134] C. Gotti,[76] E. Goudzovski,[12] C. Grace,[108] M. Graham,[143] E. Gramellini,[170] R. Gran,[118] E. Granados,[64] A. Grant,[44] C. Grant,[13] D. Gratieri,[58] P. Green,[114] S. Green,[28] L. Greenler,[169] M. Greenwood,[128] J. Greer,[14] W. C. Griffith,[153] M. Groh,[88] J. Grudzinski,[4] K. Grzelak,[165] W. Gu,[15] V. Guarino,[4] R. Guenette,[67] A. Guglielmi,[131] B. Guo,[149] K. K. Guthikonda,[65] R. Gutierrez,[3] P. Guzowski,[114] M. M. Guzzo,[29] S. Gwon,[33] A. Habig,[118] A. Hackenburg,[170] H. Hadavand,[157] R. Haenni,[10] A. Hahn,[56] J. Haigh,[166] J. Haiston,[147] T. Hamernik,[56] P. Hamilton,[85] J. Han,[136] K. Harder,[142] D. A. Harris,[172, 56] J. Hartnell,[153] T. Hasegawa,[96] R. Hatcher,[56] E. Hazen,[13] A. Heavey,[56] K. M. Heeger,[170] K. Hennessy,[109] S. Henry,[140] M. A. Hernandez Morquecho,[64] K. Herner,[56] L. Hertel,[23] A. S. Hesam,[18] J. Hewes,[34] A. Higuera,[69] T. Hill,[83] S. J. Hillier,[12] A. Himmel,[56] J. Hoff,[56] C. Hohl,[9] A. Holin,[161] E. Hoppe,[130] G. A. Horton-Smith,[98] M. Hostert,[47] A. Hourlier,[115] B. Howard,[88] R. Howell,[140] J. Huang,[158] J. Huang,[22] J. Hugon,[111] G. Iles,[85] A. M. Iliescu,[73] R. Illingworth,[56] A. Ioannisian,[171] R. Itay,[143]

A. Izmaylov,[72] E. James,[56] B. Jargowsky,[23] F. Jediny,[41] C. Jesús-Valls,[71] X. Ji,[15] L. Jiang,[164] S. Jiménez,[19] A. Jipa,[16] A. Joglekar,[25] C. Johnson,[38] R. Johnson,[34] B. Jones,[157] S. Jones,[161] C. K. Jung,[151] T. Junk,[56] Y. Jwa,[39] M. Kabirnezhad,[129] A. Kaboth,[142] I. Kadenko,[101] F. Kamiya,[54] G. Karagiorgi,[39] A. Karcher,[108] M. Karolak,[17] Y. Karyotakis,[20] S. Kasai,[100] S. P. Kasetti,[111] L. Kashur,[38] N. Kazaryan,[171] E. Kearns,[13] P. Keener,[132] K.J. Kelly,[56] E. Kemp,[29] W. Ketchum,[56] S. H. Kettell,[15] M. Khabibullin,[80] A. Khotjantsev,[80] A. Khvedelidze,[59] D. Kim,[18] B. King,[56] B. Kirby,[15] M. Kirby,[56] J. Klein,[132] K. Koehler,[169] L. W. Koerner,[69] S. Kohn,[21,108] P. P. Koller,[10] M. Kordosky,[168] T. Kosc,[81] U. Kose,[18] V. A. Kostelecký,[88] K. Kothekar,[14] F. Krennrich,[91] I. Kreslo,[10] Y. Kudenko,[80] V. A. Kudryavtsev,[146] S. Kulagin,[80] J. Kumar,[68] R. Kumar,[139] C. Kuruppu,[149] V. Kus,[41] T. Kutter,[111] A. Lambert,[108] K. Lande,[132] C. E. Lane,[45] K. Lang,[158] T. Langford,[170] P. Lasorak,[153] D. Last,[132] C. Lastoria,[19] A. Laundrie,[169] A. Lawrence,[108] I. Lazanu,[16] R. LaZur,[38] T. Le,[159] J. Learned,[68] P. LeBrun,[81] G. Lehmann Miotto,[18] R. Lehnert,[88] M. A. Leigui de Oliveira,[54] M. Leitner,[108] M. Leyton,[71] L. Li,[23] S. Li,[15] S. W. Li,[143] T. Li,[50] Y. Li,[15] H. Liao,[98] C. S. Lin,[108] S. Lin,[38] A. Lister,[169] B. R. Littlejohn,[84] J. Liu,[23] S. Lockwitz,[56] T. Loew,[108] M. Lokajicek,[40] I. Lomidze,[59] K. Long,[85] K. Loo,[95] D. Lorca,[10] T. Lord,[166] J. M. LoSecco,[126] W. C. Louis,[110] K.B. Luk,[21,108] X. Luo,[26] N. Lurkin,[12] T. Lux,[71] V. P. Luzio,[54] D. MacFarland,[143] A. A. Machado,[29] P. Machado,[56] C. T. Macias,[88] J. R. Macier,[56] A. Maddalena,[61] P. Madigan,[21,108] S. Magill,[4] K. Mahn,[117] A. Maio,[103,106] J. A. Maloney,[42] G. Mandrioli,[73] J. C. Maneira,[103,106] L. Manenti,[161] S. Manly,[140] A. Mann,[159] K. Manolopoulos,[142] M. Manrique Plata,[88] A. Marchionni,[56] W. Marciano,[15] D. Marfatia,[68] C. Mariani,[164] J. Maricic,[68] F. Marinho,[53] A. D. Marino,[37] M. Marshak,[160] C. Marshall,[108] J. Marshall,[166] J. Marteau,[81] J. Martin-Albo,[72] N. Martinez,[138] D.A. Martinez Caicedo,[147] S. Martynenko,[151] K. Mason,[159] A. T. Mastbaum,[141] M. Masud,[72] S. Matsuno,[68] J. Matthews,[111] C. Mauger,[132] N. Mauri,[73] K. Mavrokoridis,[109] R. Mazza,[76] A. Mazzacane,[56] E. Mazzucato,[17] E. McCluskey,[56] N. McConkey,[114] K. S. McFarland,[140] C. McGrew,[151] A. McNab,[114] A. Mefodiev,[80] P. Mehta,[94] P. Melas,[7] M. Mellinato,[76] O. Mena,[72] S. Menary,[172] L. Mendes Santos,[29] H. Mendez,[138] A. Menegolli,[79] G. Meng,[131] M. D. Messier,[88] W. Metcalf,[111] M. Mewes,[88] H. Meyer,[167] T. Miao,[56] G. Michna,[148] T. Miedema,[122] J. Migenda,[146] R. Milincic,[68] W. Miller,[160] J. Mills,[159] C. Milne,[83] O. Mineev,[80] O. G. Miranda,[35] S. Miryala,[15] C. S. Mishra,[56] S. R. Mishra,[149] A. Mislivec,[160] D. Mladenov,[18] I. Mocioiu,[133] K. Moffat,[47] N. Moggi,[73] R. Mohanta,[70] T. A. Mohayai,[56] N. Mokhov,[56] J. Molina,[6] L. Molina Bueno,[49] A. Montanari,[73] C. Montanari,[79] D. Montanari,[56] L. M. Montano Zetina,[35] J. Moon,[115] M. Mooney,[38] A. Moor,[28] D. Moreno,[3] B. Morgan,[166] C. Morris,[69] C. Mossey,[56] E. Motuk,[161] C. A. Moura,[54] J. Mousseau,[116] W. Mu,[56] L. Mualem,[27] J. Mueller,[38] M. Muether,[167] S. Mufson,[88] F. Muheim,[50] A. Muir,[44] M. Mulhearn,[22] H. Muramatsu,[160] S. Murphy,[49] J. Musser,[88] J. Nachtman,[90] S. Nagu,[112] M. Nalbandyan,[171] R. Nandakumar,[142] D. Naples,[136] S. Narita,[92] D. Navas-Nicolás,[19] N. Nayak,[23] M. Nebot-Guinot,[50] L. Necib,[27] K. Negishi,[92] J. K. Nelson,[168] J. Nesbit,[169] M. Nessi,[18] D. Newbold,[142] M. Newcomer,[132] D. Newhart,[56] R. Nichol,[161] E. Niner,[56] K. Nishimura,[68] A. Norman,[56] R. Northrop,[32] P. Novella,[72] J. A. Nowak,[107] M. Oberling,[4] A. Olivares Del Campo,[47] A. Olivier,[140] Y. Onel,[90] Y. Onishchuk,[101] J. Ott,[23] L. Pagani,[22] S. Pakvasa,[68] O. Palamara,[56] S. Palestini,[18] J. M. Paley,[56] M. Pallavicini,[75] C. Palomares,[19] E. Pantic,[22] V. Paolone,[136] V. Papadimitriou,[56] R. Papaleo,[152] A. Papanestis,[142] S. Paramesvaran,[14] S. Parke,[56] Z. Parsa,[15] M. Parvu,[16] S. Pascoli,[47] L. Pasqualini,[73] J. Pasternak,[85] J. Pater,[114] C. Patrick,[161] L. Patrizii,[73] R. B. Patterson,[27] S. J. Patton,[108] T. Patzak,[1] A. Paudel,[98] B. Paulos,[169] L. Paulucci,[54] Z. Pavlovic,[56] G. Pawloski,[160] D. Payne,[109] V. Pec,[146] S. J. M. Peeters,[153] Y. Penichot,[17] E. Pennacchio,[81] A. Penzo,[90] O. L. G. Peres,[29] J. Perry,[50] D. Pershey,[46] G. Pessina,[76] G. Petrillo,[143] C. Petta,[74] R. Petti,[149] F. Piastra,[10] L. Pickering,[117] F. Pietropaolo,[18,131] J. Pillow,[166] R. Plunkett,[56] R. Poling,[160] X. Pons,[18] N. Poonthottathil,[91] S. Pordes,[56] M. Potekhin,[15] R. Potenza,[74] B. V. K. S. Potukuchi,[93] J. Pozimski,[85] M. Pozzato,[73] S. Prakash,[29] T. Prakash,[108] S. Prince,[67] D. Pugnere,[81] K. Qi,[151] X. Qian,[15] J. L. Raaf,[56] R. Raboanary,[2] V. Radeka,[15] J. Rademacker,[14] B. Radics,[49] A. Rafique,[4] E. Raguzin,[15] M. Rai,[166] M. Rajaoalisoa,[34] I. Rakhno,[56] H. T. Rakotondramanana,[2] L. Rakotondravohitra,[2] Y. A. Ramachers,[166] R. Rameika,[56] M. A. Ramirez Delgado,[64] B. Ramson,[56] A. Rappoldi,[79] G. Raselli,[79] P. Ratoff,[107] S. Ravat,[18] H. Razafinime,[2] J.S. Real,[63] B. Rebel,[169,56] D. Redondo,[19] M. Reggiani-Guzzo,[29] T. Rehak,[45] J. Reichenbacher,[147] S. D. Reitzner,[56] A. Renshaw,[69] S. Rescia,[15] F. Resnati,[18] A. Reynolds,[129] G. Riccobene,[152] L. C. J. Rice,[136] K. Rielage,[110] Y. Rigaut,[49] D. Rivera,[132] L. Rochester,[143] M. Roda,[109] P. Rodrigues,[129] M. J. Rodriguez Alonso,[18] J. Rodriguez Rondon,[147] A. J. Roeth,[46] H. Rogers,[38] S. Rosauro-Alcaraz,[113] M. Rossella,[79] J. Rout,[94] S. Roy,[66] A. Rubbia,[49] C. Rubbia,[60] B. Russell,[108] J. Russell,[143] D. Ruterbories,[140] R. Saakyan,[161] S. Sacerdoti,[1] T. Safford,[117] N. Sahu,[87] P. Sala,[77,18] N. Samios,[15] M. C. Sanchez,[91] D. A. Sanders,[119] D. Sankey,[142] S. Santana,[138] M. Santos-Maldonado,[138] N. Saoulidou,[7] P. Sapienza,[152] C. Sarasty,[34] I. Sarcevic,[5] G. Savage,[56] V. Savinov,[136] A. Scaramelli,[79] A. Scarff,[146] A. Scarpelli,[1]

T. Schaffer,[118] H. Schellman,[128,56] P. Schlabach,[56] D. Schmitz,[32] K. Scholberg,[46] A. Schukraft,[56] E. Segreto,[29] J. Sensenig,[132] I. Seong,[23] A. Sergi,[12] F. Sergiampietri,[151] D. Sgalaberna,[18] M. H. Shaevitz,[39] S. Shafaq,[94] M. Shamma,[25] H. R. Sharma,[93] R. Sharma,[15] T. Shaw,[56] C. Shepherd-Themistocleous,[142] S. Shin,[32] D. Shooltz,[117] R. Shrock,[151] L. Simard,[102] N. Simos,[15] J. Sinclair,[10] G. Sinev,[46] J. Singh,[112] J. Singh,[112] R. Sipos,[18] F. W. Sippach,[39] G. Sirri,[73] A. Sitraka,[147] K. Siyeon,[33] D. Smargianaki,[151] A. Smith,[46] A. Smith,[28] E. Smith,[88] P. Smith,[88] J. Smolik,[41] M. Smy,[23] P. Snopok,[84] M. Soares Nunes,[29] H. Sobel,[23] M. Soderberg,[154] C. J. Solano Salinas,[89] S. Söldner-Rembold,[114] N. Solomey,[167] V. Solovov,[104] W. E. Sondheim,[110] M. Sorel,[72] J. Soto-Oton,[19] A. Sousa,[34] K. Soustruznik,[31] F. Spagliardi,[129] M. Spanu,[15] J. Spitz,[116] N. J. Spooner,[146] K. Spurgeon,[154] R. Staley,[12] M. Stancari,[56] L. Stanco,[131] H. M. Steiner,[108] J. Stewart,[15] B. Stillwell,[32] J. Stock,[147] F. Stocker,[18] T. Stokes,[111] M. Strait,[160] T. Strauss,[56] S. Striganov,[56] A. Stuart,[36] D. Summers,[119] A. Surdo,[144] V. Susic,[9] L. Suter,[56] C. M. Sutera,[74] R. Svoboda,[22] B. Szczerbinska,[156] A. Szelc,[114] R. Talaga,[4] H. A. Tanaka,[143] B. Tapia Oregui,[158] A. Tapper,[85] S. Tariq,[56] E. Tatar,[83] R. Tayloe,[88] A. M. Teklu,[151] M. Tenti,[73] K. Terao,[143] C. A. Ternes,[72] F. Terranova,[76] G. Testera,[75] A. Thea,[142] J. L. Thompson,[146] C. Thorn,[15] S. C. Timm,[56] A. Tonazzo,[1] M. Torti,[76] M. Tortola,[72] F. Tortorici,[74] D. Totani,[56] M. Toups,[56] C. Touramanis,[109] J. Trevor,[27] W. H. Trzaska,[95] Y. T. Tsai,[143] Z. Tsamalaidze,[59] K. V. Tsang,[143] N. Tsverava,[59] S. Tufanli,[18] C. Tull,[108] E. Tyley,[146] M. Tzanov,[111] M. A. Uchida,[28] J. Urheim,[88] T. Usher,[143] M. R. Vagins,[99] P. Vahle,[168] G. A. Valdiviesso,[51] E. Valencia,[168] Z. Vallari,[27] J. W. F. Valle,[72] S. Vallecorsa,[18] R. Van Berg,[132] R. G. Van de Water,[110] D. Vanegas Forero,[29] F. Varanini,[131] D. Vargas,[71] G. Varner,[68] J. Vasel,[88] G. Vasseur,[17] K. Vaziri,[56] S. Ventura,[131] A. Verdugo,[19] S. Vergani,[28] M. A. Vermeulen,[122] M. Verzocchi,[56] H. Vieira de Souza,[29] C. Vignoli,[61] C. Vilela,[151] B. Viren,[15] T. Vrba,[41] T. Wachala,[121] A. V. Waldron,[85] M. Wallbank,[34] H. Wang,[24] J. Wang,[22] Y. Wang,[24] Y. Wang,[151] K. Warburton,[91] D. Warner,[38] M. Wascko,[85] D. Waters,[161] A. Watson,[12] P. Weatherly,[45] A. Weber,[142,129] M. Weber,[10] H. Wei,[15] A. Weinstein,[91] D. Wenman,[169] M. Wetstein,[91] M. R. While,[147] A. White,[157] L. H. Whitehead,[28] D. Whittington,[154] M. J. Wilking,[151] C. Wilkinson,[10] Z. Williams,[157] F. Wilson,[142] R. J. Wilson,[38] J. Wolcott,[159] T. Wongjirad,[159] K. Wood,[151] L. Wood,[130] E. Worcester,[15] M. Worcester,[15] C. Wret,[140] W. Wu,[56] W. Wu,[23] Y. Xiao,[23] G. Yang,[151] T. Yang,[56] N. Yershov,[80] K. Yonehara,[56] T. Young,[123] B. Yu,[15] J. Yu,[157] J. Zalesak,[40] L. Zambelli,[20] B. Zamorano,[62] A. Zani,[77] L. Zazueta,[168] G. P. Zeller,[56] J. Zennamo,[56] K. Zeug,[169] C. Zhang,[15] M. Zhao,[15] E. Zhivun,[15] G. Zhu,[127] E. D. Zimmerman,[37] M. Zito,[17] S. Zucchelli,[73] J. Zuklin,[40] V. Zutshi,[124] and R. Zwaska[56]

(The DUNE Collaboration)

[1] *APC - Université de Paris, CNRS/IN2P3, CEA/lrfu, Observatoire de Paris, 10, rue Alice Domon et Léonie Duquet, 75205 Paris Cedex 13, France*
[2] *University of Antananarivo, BP 566, Antananarivo 101, Madagascar*
[3] *Universidad Antonio Nariño, Cra 3 Este No 47A-15, Bogotá, Colombia*
[4] *Argonne National Laboratory, Argonne, IL 60439, USA*
[5] *University of Arizona, 1118 E. Fourth Street Tucson, AZ 85721, USA*
[6] *Universidad Nacional de Asunción, San Lorenzo, Paraguay*
[7] *University of Athens, University Campus, Zografou GR 157 84, Greece*
[8] *Universidad del Atlantico, Carrera 30 Número 8- 49 Puerto Colombia - Atlántico, Colombia*
[9] *University of Basel, Klingelbergstrasse 82, CH-4056 Basel, Switzerland*
[10] *University of Bern, Sidlerstrasse 5, CH-3012 Bern, Switzerland*
[11] *Beykent University, Istanbul*
[12] *University of Birmingham, Edgbaston, Birmingham B15 2TT, United Kingdom*
[13] *Boston University, Boston, MA 02215, USA*
[14] *University of Bristol, H. H. Wills Physics Laboratory, Tyndall Avenue Bristol BS8 1TL, United Kingdom*
[15] *Brookhaven National Laboratory, Upton, NY 11973, USA*
[16] *University of Bucharest, Faculty of Physics, Bucharest, Romania*
[17] *CEA/Saclay, IRFU Institut de Recherche sur les Lois Fondamentales de l'Univers, F-91191 Gif-sur-Yvette CEDEX, France*
[18] *CERN, European Organization for Nuclear Research 1211 Genève 23, Switzerland, CERN*
[19] *CIEMAT, Centro de Investigaciones Energéticas, Medioambientales y Tecnológicas, Av. Complutense, 40, E-28040 Madrid, Spain*
[20] *Laboratoire d'Annecy-le-Vieux de Physique des Particules, CNRS/IN2P3 and Université Savoie Mont Blanc, CNRS/IN2P3 and Université Savoie Mont Blanc, 74941 Annecy-le-Vieux, France*
[21] *University of California Berkeley, Berkeley, CA 94720, USA*
[22] *University of California Davis, Davis, CA 95616, USA*
[23] *University of California Irvine, Irvine, CA 92697, USA*
[24] *University of California Los Angeles, Los Angeles, CA 90095, USA*
[25] *University of California Riverside, 900 University Ave, Riverside CA 92521*
[26] *University of California Santa Barbara, Santa Barbara, California 93106 USA*

[27]California Institute of Technology, Pasadena, CA 91125, USA
[28]University of Cambridge, JJ Thomson Avenue, Cambridge CB3 0HE, United Kingdom
[29]Universidade Estadual de Campinas, Campinas - SP, 13083-970, Brazil
[30]Centro Brasileiro de Pesquisas Físicas, Rio de Janeiro, RJ 22290-180, Brazil
[31]Institute of Particle and Nuclear Physics of the Faculty of Mathematics and Physics of the Charles University in Prague, V Holešovičkách 747/2, 180 00 Praha 8-Libeň, Czech Republic
[32]University of Chicago, Chicago, IL 60637, USA
[33]Chung-Ang University, Dongjak-Gu, Seoul 06974, South Korea
[34]University of Cincinnati, Cincinnati, OH 45221, USA
[35]Centro de Investigacion y de Estudios Avanzados del IPN (Cinvestav), Mexico City
[36]Universidad de Colima, 340 Colonia Villa San Sebastian Colima, Colima, Mexico
[37]University of Colorado Boulder, Boulder, CO 80309, USA
[38]Colorado State University, Fort Collins, CO 80523, USA
[39]Columbia University, New York, NY 10027, USA
[40]Institute of Physics, Czech Academy of Sciences, Na Slovance 2, 182 21 Praha 8, Czech Republic
[41]Czech Technical University in Prague, Břehová 78/7, 115 19 Prague 1, Czech Republic
[42]Dakota State University, Madison, SD 57042, USA
[43]University of Dallas, Irving, TX 75062-4736, USA
[44]Daresbury Laboratory, Daresbury Warrington, Cheshire WA4 4AD, United Kingdom
[45]Drexel University, Philadelphia, PA 19104, USA
[46]Duke University, Durham, NC 27708, USA
[47]Durham University, South Road, Durham DH1 3LE, United Kingdom
[48]Universidad EIA, Via José María Córdoba #km 2 + 200, Envigado, Antioquia
[49]ETH Zurich, Institute for Particle Physics, Zurich, Switzerland
[50]University of Edinburgh, Edinburgh EH8 9YL, United Kingdom
[51]Universidade Federal de Alfenas, Poços de Caldas - MG, 37715-400, Brazil
[52]Universidade Federal de Goias, Goiania, GO 74690-900, Brazil
[53]Universidade Federal de São Carlos, Araras - SP, 13604-900, Brazil
[54]Universidade Federal do ABC, Av. dos Estados 5001, Santo André - SP, 09210-580 Brazil
[55]Universidade Federal do Rio de Janeiro, Rio de Janeiro - RJ, 21941-901, Brazil
[56]Fermi National Accelerator Laboratory, Batavia, IL 60510
[57]University of Florida, PO Box 118440 Gainesville, FL 32611-8440, USA
[58]Fluminense Federal University, Rua Miguel de Frias, 9 Icaraí Niterói - RJ, 24220-900, Brazil
[59]Georgian Technical University, 77 Kostava Str. 0160, Tbilisi, Georgia
[60]Gran Sasso Science Institute, Viale Francesco Crispi 7, L'Aquila, Italy
[61]Laboratori Nazionali del Gran Sasso, I-67010 Assergi, AQ, Italy
[62]University of Granada & CAFPE, Campus Fuentenueva (Edif. Mecenas), 18002 Granada, Spain
[63]University Grenoble Alpes, CNRS, Grenoble INP, LPSC-IN2P3, 38000 Grenoble, France
[64]Universidad de Guanajuato, Gto., C.P. 37000, Mexico
[65]Department of Physics, K L E F, Green Fields, Guntur - 522 502, AP, India
[66]Harish-Chandra Research Institute, Jhunsi, Allahabad 211 019, India
[67]Harvard University, 17 Oxford St. Cambridge, MA 02138, USA
[68]University of Hawaii, Honolulu, HI 96822, USA
[69]University of Houston, Houston, TX 77204, USA
[70]University of Hyderabad, Gachibowli, Hyderabad - 500 046, India
[71]Institut de Fìsica d'Altes Energies, Barcelona i.e. Catalan ersitat Autonoma de Barcelona, Campus UAB, Facultat Ciències Nord, 08193 Bellaterra, Barcelona, Spain
[72]Instituto de Fisica Corpuscular, Catedratico Jose Beltran, 2 E-46980 Paterna (Valencia), Spain
[73]Istituto Nazionale di Fisica Nucleare Bologna, 40127 Bologna BO, Italy
[74]Istituto Nazionale di Fisica Nucleare Sezione di Catania, Via Santa Sofia 64, I-95123 Catania, Italy
[75]Università degli studi di Genova, Istituto Nazionale di Fisica Nucleare Genova, 16126 Genova GE, Italy
[76]Istituto Nazionale di Fisica Nucleare Sezione di Milano Bicocca and University of Milano Bicocca, Piazza della Scienza, 3 - I-20126 Milano, Italy
[77]Istituto Nazionale di Fisica Nucleare Milano, I-20133 Milano, Italy
[78]Istituto Nazionale di Fisica Nucleare - Sezione di Napoli, Complesso Universitario di Monte S. Angelo, I-80126 Napoli, Italy
[79]Università degli studi di Pavia, Istituto Nazionale di Fisica Nucleare Sezione di Pavia, I-27100 Pavia, Italy
[80]Institute for Nuclear Research of the Russian Academy of Sciences , prospekt 60-letiya Oktyabrya 7a, Moscow 117312, Russia
[81]Institut de Physique des 2 Infinis de Lyon, Rue E. Fermi 4 69622 Villeurbanne, France
[82]Institute for Research in Fundamental Sciences , Farmanieh St. Tehran, 19538-33511, Iran
[83]Idaho State University, Department of Physics, Pocatello, ID 83209, USA
[84]Illinois Institute of Technology, Chicago, IL 60616, USA
[85]Imperial College of Science Technology and Medicine, Blackett Laboratory Prince Consort Road, London SW7 2BZ, United Kingdom
[86]Indian Institute of Technology Guwahati, Guwahati, 781 039, India

[87]*Indian Institute of Technology Hyderabad, Hyderabad, 502285, India*
[88]*Indiana University, Bloomington, IN 47405, USA*
[89]*Universidad Nacional de Ingeniería, Av. Tupac Amaru 210, Lima 25, Perú*
[90]*University of Iowa, Department of Physics and Astronomy 203 Van Allen Hall Iowa City, IA 52242, USA*
[91]*Iowa State University, Ames, Iowa 50011, USA*
[92]*Iwate University, Morioka, Iwate 020-8551, Japan*
[93]*University of Jammu, Physics Department, JAMMU-180006, India*
[94]*Jawaharlal Nehru University, School of Physical Sciences, New Delhi 110067, India*
[95]*University of Jyvaskyla, P.O. Box 35, FI-40014, Finland*
[96]*High Energy Accelerator Research Organization (KEK), Ibaraki, 305-0801, Japan*
[97]*Korea Institute of Science and Technology Information, Daejeon, 34141, South Korea*
[98]*Kansas State University, Manhattan, KS 66506, USA*
[99]*Kavli Institute for the Physics and Mathematics of the Universe , Kashiwa, Chiba 277-8583, Japan*
[100]*National Institute of Technology, Kure College, Hiroshima, 737-8506, Japan*
[101]*Kyiv National University, 64, 01601 Kyiv, Ukraine*
[102]*Laboratoire de l'Accélérateur Linéaire , Bâtiment 200, 91440 Orsay, France*
[103]*Laboratório de Instrumentação e Física Experimental de Partículas - LIP, Lisboa, Portugal*
[104]*Laboratório de Instrumentação e Física Experimental de Partículas - LIP, Coimbra, Portugal*
[105]*Instituto Superior Técnico - IST, Universidade de Lisboa, Portugal*
[106]*Faculdade de Ciências - FCUL, Universidade de Lisboa, Portugal*
[107]*Lancaster University, Bailrigg, Lancaster LA1 4YB, United Kingdom*
[108]*Lawrence Berkeley National Laboratory, Berkeley, CA 94720, USA*
[109]*University of Liverpool, L69 7ZE, Liverpool, United Kingdom*
[110]*Los Alamos National Laboratory, Los Alamos, NM 87545, USA*
[111]*Louisiana State University, Baton Rouge, LA 70803, USA*
[112]*University of Lucknow, Lucknow 226007, Uttar Pradesh, India*
[113]*Madrid Autonoma University and IFT UAM/CSIC, Ciudad Universitaria de Cantoblanco 28049 Madrid, Spain*
[114]*University of Manchester, Oxford Road, Manchester M13 9PL, United Kingdom*
[115]*Massachusetts Institute of Technology, Cambridge, MA 02139, USA*
[116]*University of Michigan, Ann Arbor, MI 48109, USA*
[117]*Michigan State University, East Lansing, MI 48824, USA*
[118]*University of Minnesota Duluth, Duluth, MN 55812, USA*
[119]*University of Mississippi, P.O. Box 1848, University, MS 38677 USA*
[120]*University of New Mexico, 1919 Lomas Blvd. N.E. Albuquerque, NM 87131, USA*
[121]*H. Niewodniczański Institute of Nuclear Physics, Polish Academy of Sciences, Cracow, Poland*
[122]*Nikhef National Institute of Subatomic Physics, Science Park, Amsterdam, Netherlands*
[123]*University of North Dakota, 3501 University Ave Grand Forks, ND 58202-8357, USA*
[124]*Northern Illinois University, Department of Physics, DeKalb, Illinois 60115, USA*
[125]*Northwestern University, Evanston, Il 60208, USA*
[126]*University of Notre Dame, Notre Dame, IN 46556, USA*
[127]*Ohio State University, 191 W. Woodruff Ave. Columbus, OH 43210, USA*
[128]*Oregon State University, Corvallis, OR 97331, USA*
[129]*University of Oxford, Oxford, OX1 3RH, United Kingdom*
[130]*Pacific Northwest National Laboratory, Richland, WA 99352, USA*
[131]*Universtà Degli Studi di Padova, Dip. Fisica e Astronomia G. Galilei and INFN Sezione di Padova, I-35131 Padova, Italy*
[132]*University of Pennsylvania, Philadelphia, PA 19104, USA*
[133]*Pennsylvania State University, University Park, PA 16802, USA*
[134]*Physical Research Laboratory, Ahmedabad 380 009, India*
[135]*Università di Pisa, Theor. Division; Largo B. Pontecorvo 3, Ed. B-C, I-56127 Pisa, Italy*
[136]*University of Pittsburgh, Pittsburgh, PA 15260, USA*
[137]*Pontificia Universidad Católica del Perú, Apartado 1761, Lima, Perú*
[138]*University of Puerto Rico, Mayaguez, 00681, USA*
[139]*Punjab Agricultural University, Department of Math. Stat. & Physics, Ludhiana 141004, India*
[140]*University of Rochester, Rochester, NY 14627, USA*
[141]*Rutgers University, Piscataway, NJ, 08854, USA*
[142]*STFC Rutherford Appleton Laboratory, OX11 0QX Harwell Campus, Didcot, United Kingdom*
[143]*SLAC National Acceleratory Laboratory, Menlo Park, CA 94025, USA*
[144]*Università del Salento and Istituto Nazionale Fisica Nucleare, Via Provinciale per Arnesano, 73100 Lecce, Italy*
[145]*Universidad Sergio Arboleda, Cll 74 -14 -14, 11022 Bogotá, Colombia*
[146]*University of Sheffield, Department of Physics and Astronomy, Sheffield S3 7RH, United Kingdom*
[147]*South Dakota School of Mines and Technology, Rapid City, SD 57701, USA*
[148]*South Dakota State University, Brookings, SD 57007, USA*
[149]*University of South Carolina, Columbia, SC 29208, USA*
[150]*Southern Methodist University, Dallas, TX 75275, USA*

[151] *Stony Brook University, SUNY, Stony Brook, New York 11794, USA*
[152] *INFN - Laboratori Nazionali del Sud (LNS), Via S. Sofia 62, 95123 Catania, Italy*
[153] *University of Sussex, Brighton, BN1 9RH, United Kingdom*
[154] *Syracuse University, Syracuse, NY 13244, USA*
[155] *University of Tennessee at Knoxville, TN, 37996, USA*
[156] *Texas A&M University (Corpus Christi), Corpus Christi, TX 78412, USA*
[157] *University of Texas at Arlington, Arlington, TX 76019, USA*
[158] *University of Texas at Austin, Austin, TX 78712, USA*
[159] *Tufts University, Medford, MA 02155, USA*
[160] *University of Minnesota Twin Cities, Minneapolis, MN 55455, USA*
[161] *University College London, London, WC1E 6BT, United Kingdom*
[162] *Valley City State University, Valley City, ND 58072, USA*
[163] *Variable Energy Cyclotron Centre, 1/AF, Bidhannagar Kolkata - 700 064 West Bengal, India*
[164] *Virginia Tech, Blacksburg, VA 24060, USA*
[165] *University of Warsaw, Faculty of Physics ul. Pasteura 5 02-093 Warsaw, Poland*
[166] *University of Warwick, Coventry CV4 7AL, United Kingdom*
[167] *Wichita State University, Physics Division, Wichita, KS 67260, USA*
[168] *William and Mary, Williamsburg, VA 23187, USA*
[169] *University of Wisconsin Madison, Madison, WI 53706, USA*
[170] *Yale University, New Haven, CT 06520, USA*
[171] *Yerevan Institute for Theoretical Physics and Modeling, Halabian Str. 34, Yerevan 0036, Armenia*
[172] *York University, Physics and Astronomy Department, 4700 Keele St. Toronto M3J 1P3, Canada*

Contents

Contents i

List of Figures ii

List of Tables 1

A Roadmap of the DUNE Technical Design Report 1

1 The DUNE Near Detector 2

1.1 Overview of the DUNE Near Detector 2

1.1.1 Motivation 2

1.1.2 Requirements 3

1.1.3 Design 4

1.2 Role of the ND in the DUNE Oscillation Program 8

1.3 ND Hall and Construction 12

Glossary 14

References 17

List of Figures

1.1 ArgonCube 2×2 demonstrator module 5
1.2 MPD ECAL conceptual design 6
1.3 Conceptual layout of the MPD ECAL 7
1.4 Variation of neutrino energy spectrum as function of off-axis angle 8
1.5 Linear combinations of off-axis fluxes giving FD oscillated spectra 9
1.6 The SAND detector configuration 10
1.7 DUNE near detector hall and detectors, plan view 13

List of Tables

1.1 Components of the DUNE ND 4

Chapter 1

The DUNE Near Detector

This chapter briefly introduces the DUNE near detector, emphasizing its role for the DUNE far detector physics program. More details on the near detector may be found in appendices of this TDR volume. DUNE will issue a complete conceptual design report for the near detector in early 2020, with a technical design report to follow.

1.1 Overview of the DUNE Near Detector

1.1.1 Motivation

The Deep Underground Neutrino Experiment (DUNE) experiment will measure oscillation probabilities for muon neutrinos or antineutrinos to either remain the same flavor or oscillate into their electron flavor counterparts as a function of the neutrino energy. This will allow the neutrino mass ordering to be definitively determined, as well as enable observation of leptonic charge-parity symmetry violation (CPV) for a significant range of δ_{CP} values and precise measurement of neutrino mixing matrix parameters.

The near detector (ND) will serve as the experiment's control, constraining systematic errors and measuring the initial unoscillated ν_μ and ν_e energy spectra (and that of the corresponding antineutrinos). The energy spectra result from an energy-dependent convolution of flux, cross section, and detector response for each of the four neutrino types (ν_e, ν_μ, $\bar{\nu}_e$, $\bar{\nu}_\mu$). The ND will make measurements that allow the three functions to be independently constrained and partially or fully deconvolved. The constraints will be used to improve the simulation program that is responsible for predicting the energy spectra at the far detector (FD) for particular choices of the oscillation parameters. This allows the actual oscillation parameters to be estimated from a fit to the FD data.

The ND will also have a physics program of its own, independent of the far detector. This

program will include measuring neutrino interactions to explore the two pillars of the standard model: electroweak physics and quantum chromodynamics. The ND physics program will also explore physics beyond the standard model. This includes searches for non-standard interactions, sterile neutrinos, dark photons, and other exotic particles.

1.1.2 Requirements

The components of the ND must address their multiple missions in a complementary fashion. In this section, we list the key overarching requirements driving the ND complex. Section **??** in Appendix **??** goes into more detail, discussing some thought experiments and case studies that illustrate how different parts of the complex work together. These case studies naturally suggest more detailed capabilities, performance statistics, and technical requirements; we are in the process of tabulating them.

- *Predict the neutrino spectrum at the FD.* The ND must predict the energy spectrum of ν_μ, $\bar{\nu}_\mu$, ν_e and $\bar{\nu}_e$ at the FD. The prediction must be provided as a function of the oscillation parameters, and systematic uncertainties must be small enough to achieve the required charge parity (CP) coverage. This is the primary requirement of the DUNE ND.
- *Measure interactions on argon.* The ND must measure neutrino interactions on argon to reduce uncertainties due to nuclear modeling. The ND must be able to determine the neutrino flavor and measure the full kinematic range of the interactions that will be seen at the FD.
- *Measure the neutrino energy.* The ND must be able to reconstruct the neutrino energy in charged current (CC) events and control for any biases in energy scale or resolution, keeping them small enough to achieve the required CP coverage. These measurements must also be transferable to the FD.
- *Constrain the cross section model.* The ND must measure neutrino cross sections in order to constrain the cross section model used in the oscillation analysis. In particular, cross section mismodeling that causes incorrect FD predictions as a function of neutrino flavor and true or reconstructed energy must be constrained well enough to achieve the required CP coverage.
- *Measure neutrino fluxes.* The ND must measure neutrino fluxes as a function of flavor and neutrino energy. This allows neutrino cross sections to be measured and constrains the beam model and the extrapolation of neutrino energy spectra from the ND to the FD.
- *Obtain data with different fluxes.* The ND must measure neutrino interactions in different beam fluxes (especially ones with different mean energies) to disentangle flux and cross section, verify the beam model, and guard against systematic uncertainties on the neutrino energy reconstruction.
- *Monitor the neutrino beam.* The ND must monitor the neutrino beam energy spectrum with sufficient statistics to be sensitive to intentional or accidental changes in the beam that could affect the oscillation measurement.

1.1.3 Design

The DUNE ND is formed from three primary detector components and the capability of two of these components to move off the beam axis. The three detector components serve important individual and overlapping functions in the ND mission. Because these components have stand-alone features, the DUNE ND is often discussed as a suite or complex of detectors and capabilities. The movement off-axis provides a valuable extra degree of freedom in the data. The power in the DUNE ND concept lies in the collective set of capabilities.

Figure **??** in Chapter **??** shows the DUNE ND in the DUNE ND hall. Table 1.1 provides a high-level overview of the three components of the DUNE ND along with the off-axis capability that is sometimes described as a fourth component.

Table 1.1: High-level breakdown of the three major detector components and the capability of movement for the DUNE ND, along with functions and primary physics goals.

Component	Essential Characteristics	Primary function	Select physics aims
LArTPC (ArgonCube)	Mass	Experimental control for the FD.	$\nu_\mu(\overline{\nu}_\mu)$ CC
	Target nucleus Ar	Unoscillated E_ν spectra measurements.	ν-e$^-$ scattering
	Technology FD-like	Flux determination.	ν_e+$\overline{\nu}_e$ CC Interaction model
Multipurpose detector (MPD)	Magnetic field	Experimental control for the LArTPCs.	$\nu_\mu(\overline{\nu}_\mu)$ CC
	Target nucleus Ar	Momentum-analyze μ's produced in LAr.	ν_e CC, $\overline{\nu}_e$
	Low density	Measure exclusive final states with low momentum threshold.	Interaction model
DUNE-PRISM (capability)	ArgonCube+MPD move off-axis	Change flux spectrum	Deconvolve flux $\times$ cross section; Energy response; Provide FD-like energy spectrum at ND; ID mismodeling.
Beam Monitor (SAND)	On-axis	Beam flux monitor	On-axis flux stability
	High-mass polystyrene target	Neutrons	Interaction model;
	KLOE magnet		Atomic number (A) dependence; ν-e$^-$ scattering.

The core part of the DUNE ND is a liquid argon time-projection chamber (LArTPC) called

ArgonCube. ArgonCube consists of an array of 35 modular time projection chambers (TPCs) sharing a cryostat. Figure 1.1 is a drawing of a prototype of the modular TPCs. This detector has the same target nucleus as the FD and shares some aspects of form and functionality with it, where the differences are necessitated by the expected intensity of the beam at the ND. This similarity in target nucleus and technology reduces sensitivity to nuclear effects and detector-driven systematic errors in the extraction of the oscillation signal at the FD. The LArTPC is large enough to provide high statistics ($10^8 \nu_\mu$-CC events/year) and its volume is sufficient to provide good hadron containment. The tracking and energy resolution, combined with the mass of the LArTPC, will allow the flux in the beam to be measured using several techniques, including the well understood but rare process of ν_μ-e^- scattering.

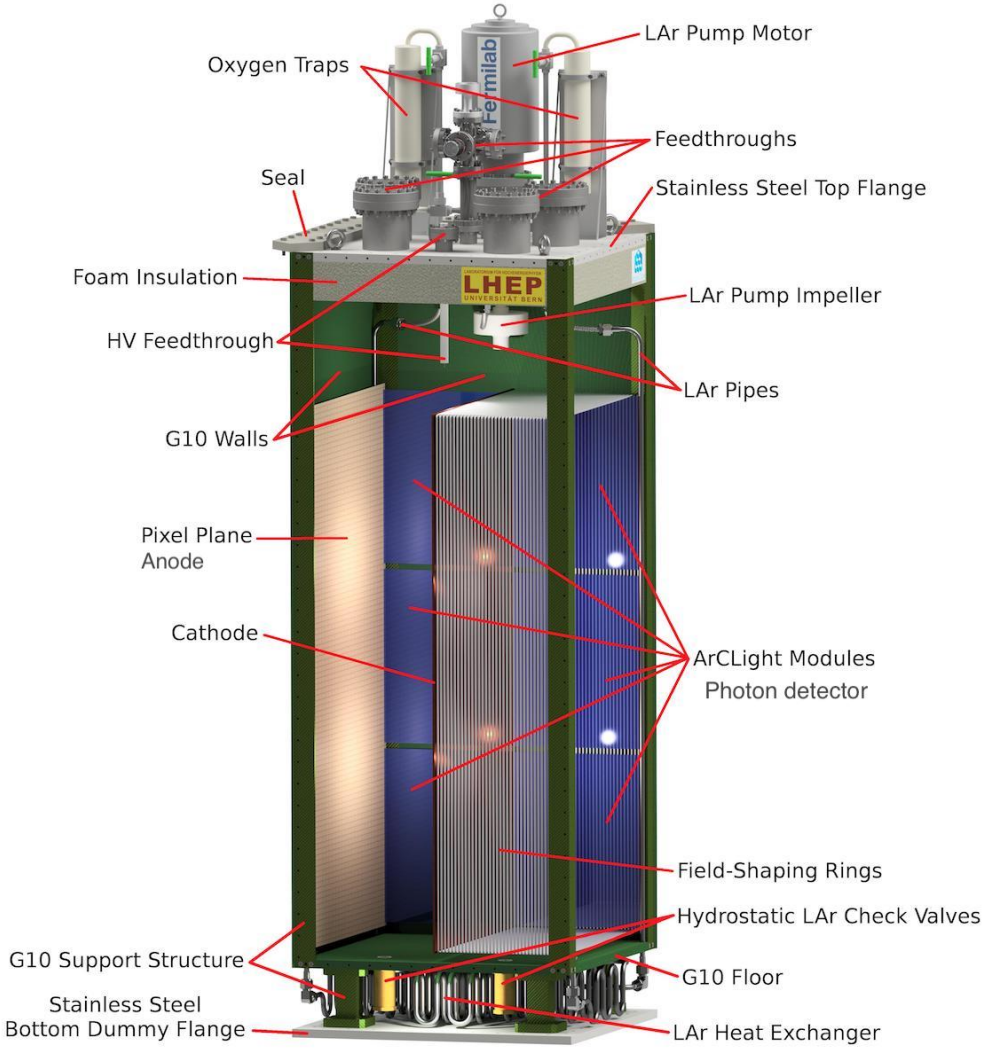


Figure 1.1: Cutaway drawing of a 0.67 m × 0.67 m × 1.81 m ArgonCube prototype module. For illustrative purposes, the drawing shows traditional field-shaping rings instead of a resistive field shell. The G10 walls will completely seal the module, isolating it from the neighboring modules and the outer liquid argon (LAr) bath. The modules in this prototype system will not have individual pumps and filters.

The LArTPC acceptance falls off for muons with a measured momentum higher than 0.7 GeV/c due to lack of containment. Since the muon momentum is a critical component of the neutrino energy determination, a magnetic spectrometer is needed downstream of the LArTPC to mea-

sure the charge sign and momentum of these muons. The multi-purpose detector (MPD) will accomplish this. It consists of a high-pressure gaseous argon TPC (HPgTPC) surrounded by an electromagnetic calorimeter (ECAL) in a 0.5 T magnetic field (Figures 1.2 and 1.3).

The HPgTPC provides a lower-density medium with excellent tracking resolution for the muons from the LArTPC. In addition, with this choice of technology for the tracker, neutrinos interacting on the argon in the gas TPC constitute a sample of ν-Ar events that can be studied with a very low charged-particle tracking threshold, excellent kinematic resolution, and systematic errors that differ from those of the liquid detector. The detector's high pressure will allow us to collect a sample of 2×10^6 ν_μ-CC events/year for these studies, events that will also be valuable for studying the charged particle activity near the interaction vertex since this detector can access lower-momentum protons than the LAr detector and provides better particle identification of charged pions. The relative reduction in secondary interactions in these samples (compared to LAr) will help us to identify the particles produced in the primary interaction and to model secondary interactions in denser detectors, interactions that are known to be important [1]. In addition, using the ECAL we will be able to reconstruct many neutrons produced in neutrino interactions in the gaseous argon via time-of-flight.

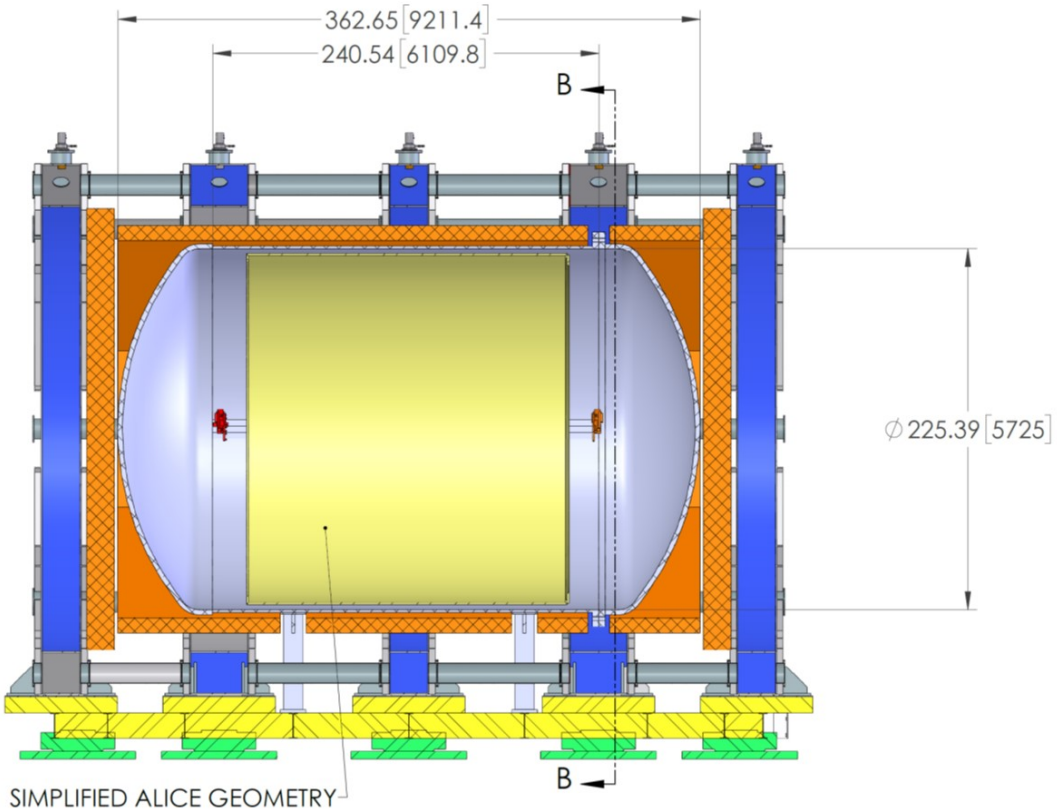


Figure 1.2: The conceptual design of the MPD system for the ND. The TPC is shown in yellow inside the pressure vessel. Outside the pressure vessel, the ECAL is shown in orange, and outside that are the magnet coils and cryostats. The drawing illustrates the five-coil superconducting design.

The LArTPC and MPD are able to move laterally to take data in positions off the beam axis. This capability is referred to as DUNE Precision Reaction-Independent Spectrum Measurement (DUNE-PRISM). As the detectors move off-axis, the incident neutrino flux spectrum changes:

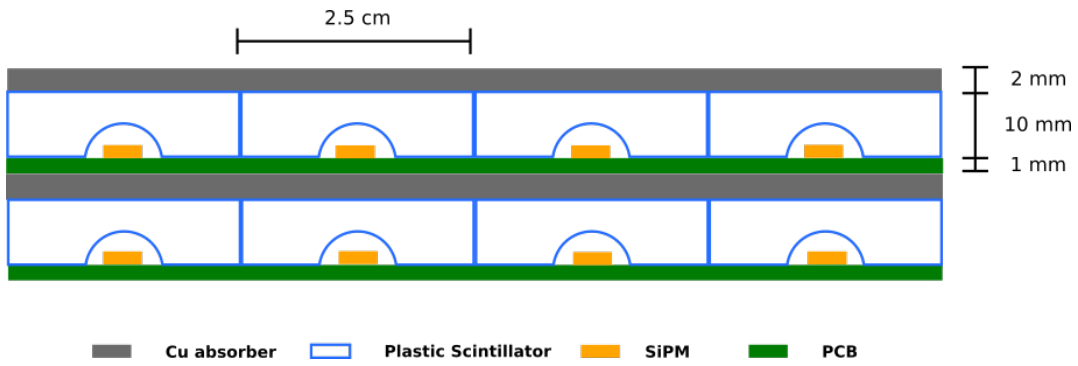


Figure 1.3: Conceptual layout of the calorimeter showing the absorber structure, scintillator tiles, silicon photomultipliers (SiPMs), and PCB. The scintillating layers consist of a mix of tiles and cross-strips with embedded wavelength shifting fibers to achieve a comparable effective granularity.

the mean energy drops and the spectrum becomes more monochromatic. Although the neutrino interaction rate drops, the intensity of the beam and the size of the LArTPC still combine to yield ample statistics. Figure 1.4 shows a sample of neutrino energy distributions taken at different off-axis angles. Taking data at different off-axis angles allows the deconvolution of the neutrino flux and interaction cross section; it also allows mapping of the reconstructed versus true energy response of the detector. This latter mapping is applicable at the FD to the degree to which the near and far LAr detectors are similar. Stated a different way, it is possible to use information from a linear combination of the different fluxes to create a data sample at the ND with an effective neutrino energy distribution close to the oscillated spectrum at the FD. This data-driven technique will reduce systematic effects coming from differences in the energy spectra of the oscillated signal events in the FD and the ND samples used to constrain the interaction model. Finally, the off-axis degree of freedom may enable a sensitivity to some forms of mismodeling in the beam and/or interaction models.

Figure 1.5 shows linear combinations of off-axis fluxes giving FD oscillated spectra for two sets of oscillation parameters. The procedure can model the FD flux well for neutrino energies in the range of 0.6 GeV to 3.6 GeV. The input spectra for the linear combinations, shown in Figure 1.4, extend only slightly outside this range; they cannot be combined to model the flux in those extreme ranges while simultaneously fitting the central range well. The modeled range encompasses the range of data of interest for the oscillation program.

The final component of the DUNE ND suite is the beam monitor, called the System for on-Axis Neutrino Detection (SAND). The core part of it, the 3D scintillator tracker (3DST), is a plastic scintillator detector made of 1 cm^3 cubes read out along each of three orthogonal dimensions. The design eliminates the typical planar-strip geometry common to scintillator detectors, leading to improved acceptance at large angles relative to the beam direction. It is mounted inside an envelope of high-resolution, normal pressure TPCs and an ECAL, all of which are surrounded by a magnet, as illustrated in Figure 1.6. The reference design uses a repurposed magnet and ECAL from the KLOE experiment.

SAND serves as a dedicated neutrino spectrum monitor that never moves off-axis. It also provides an excellent on-axis, neutrino flux determination using many of the methods discussed in Section **??**. The neutrino flux determined using this detector, with technologies, targets, and inter-

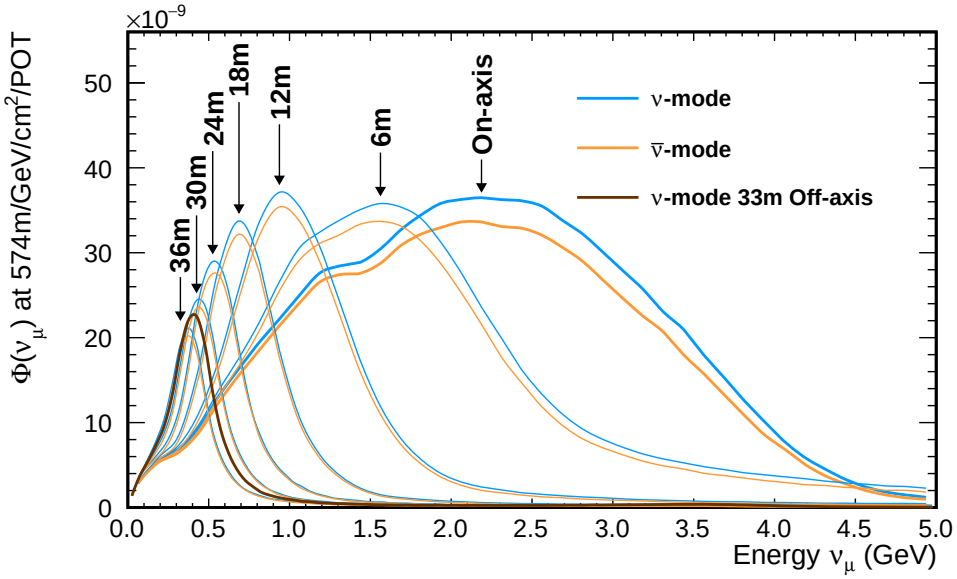


Figure 1.4: The variation in the neutrino energy spectrum shown as a function of detector off-axis position, assuming the nominal ND location 574 m downstream from the production target.

action systematic errors that are different from ArgonCube, is an important point of comparison and a systematic cross-check for the flux as determined by ArgonCube.

SAND provides very fast timing and can isolate small energy depositions from neutrons in three dimensions. This provides the capability to incorporate neutrons in the event reconstruction using energy determination via time-of-flight with a high efficiency. This capability should be useful for the low-ν flux determination[1] because it either allows events to be tagged with a significant neutron energy component or provides a way to include that energy in the calculation. Including neutrons in detailed studies of neutrino interactions in SAND using single transverse variables may prove useful in motivating improvements in the neutrino interaction model. Although the target for this device is carbon, not argon, basic insights into components of the interaction model may extend to argon. For example, the multi-nucleon component of the interaction model will be used for argon although it was developed in response to observations made on plastic targets.

1.2 Role of the ND in the DUNE Oscillation Program

Neutrino oscillation experiments must accomplish three main tasks. First, they must identify the flavor of interacting neutrinos in CC events or identify the events as neutral current (NC) interactions. Second, they must measure the energy of the neutrinos because oscillations occur as a function of baseline length over neutrino energy, L/E. Third, they must compare the observed event spectrum in the FD to predictions based on differing sets of oscillation parameters, subject to

[1]The low-ν technique involves measuring the flux for events with low energy transfer because the cross section is approximately constant with energy for this sample. It provides a nice way to measure the shape of the spectrum. This is discussed further in Section **??** of Appendix **??**.

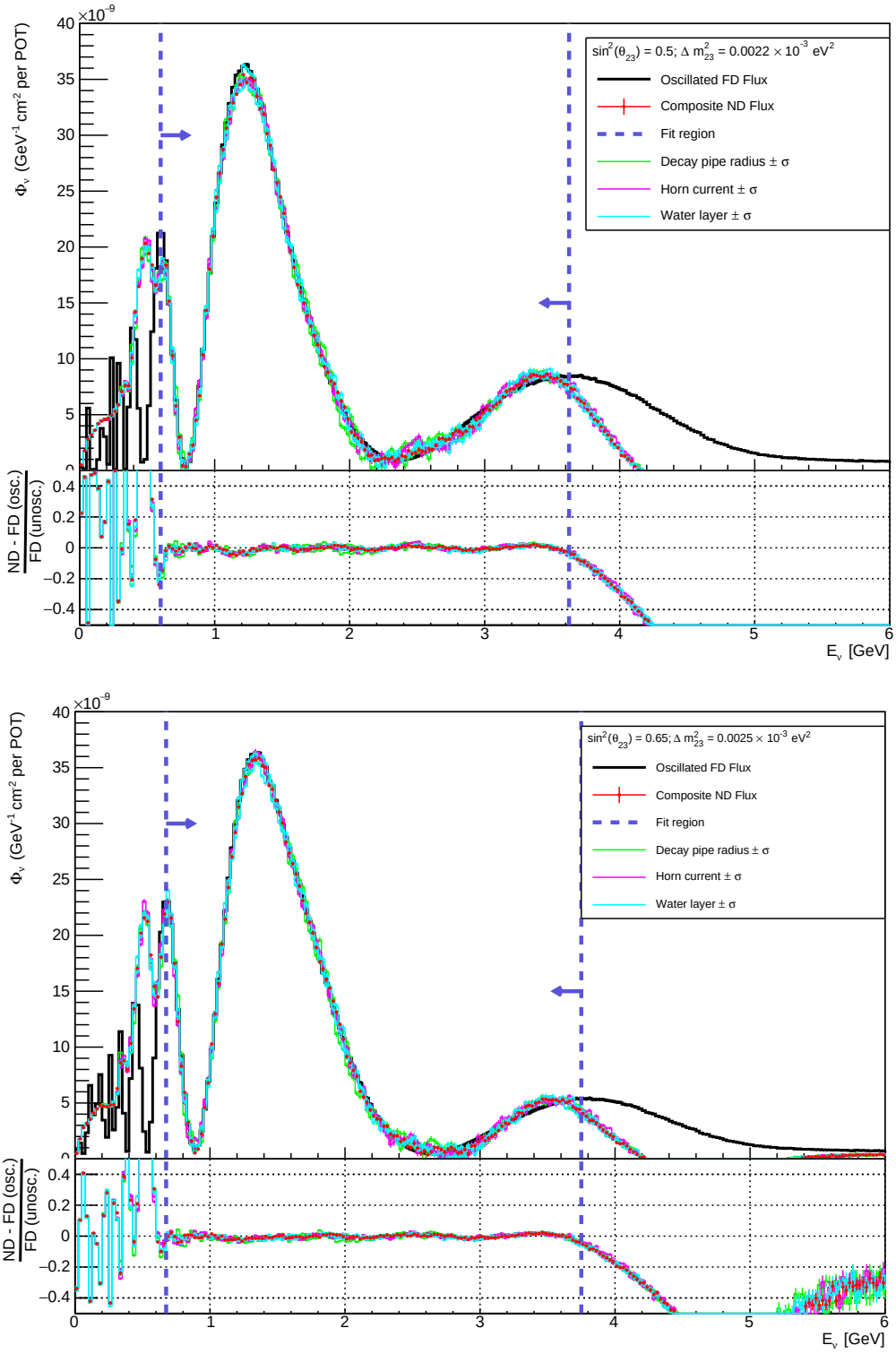


Figure 1.5: Linear combinations of off-axis fluxes giving FD oscillated spectra for a range of oscillation parameters. The FD oscillated flux is shown in black, the target flux is shown in green, and the linearly combined flux obtained with the nominal beam Monte Carlo (MC) is shown in red. Systematic effects due to $1\,\sigma$ variations of the decay pipe radius (green), horn current (magenta), and horn cooling water layer thickness (teal) are also shown.

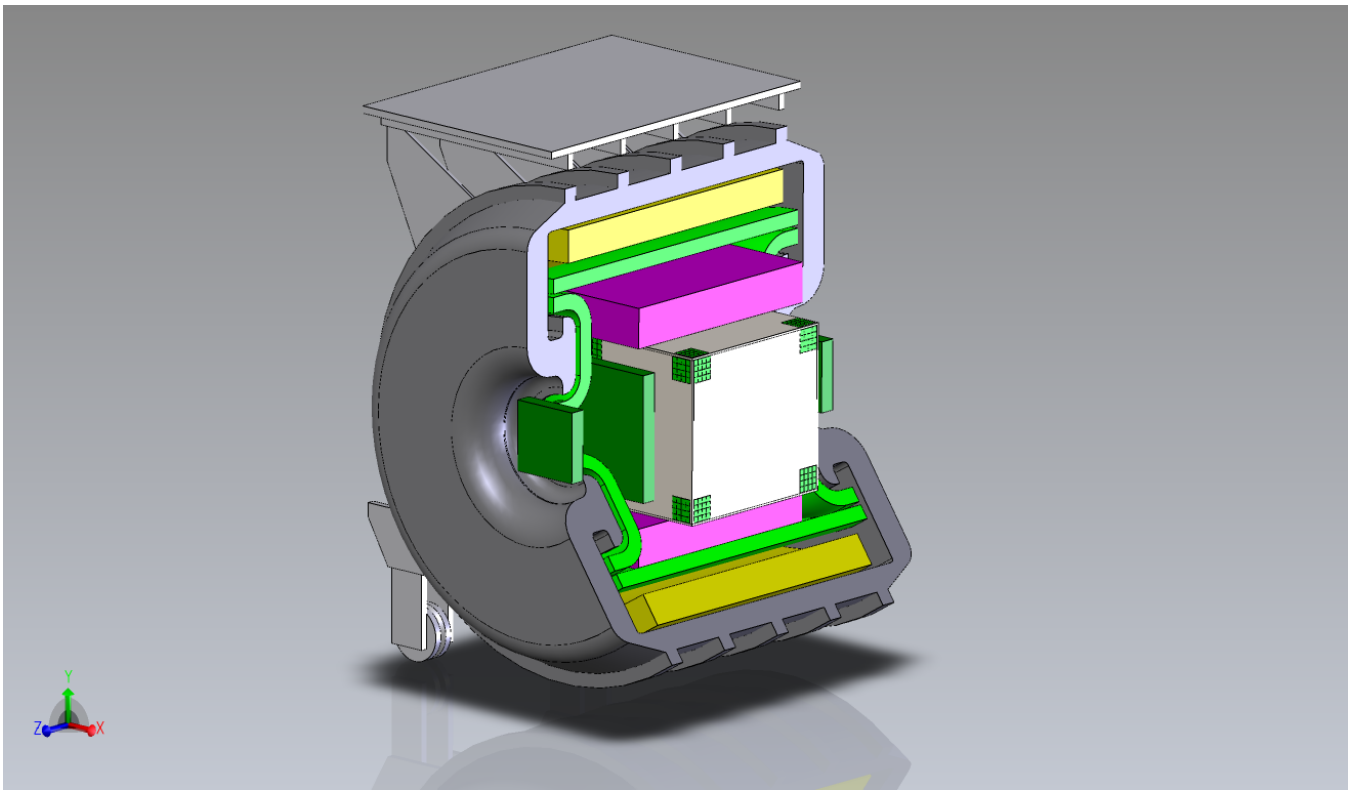


Figure 1.6: The SAND detector configuration with the 3DST inside the KLOE magnet. The drawing shows the 3DST in the center (white), TPCs (magenta), ECAL (green), magnet coil (yellow), and the return yoke (gray).

constraints from data observed in the ND. That comparison and how it varies with the oscillation parameters allows oscillation parameters to be measured.

The connection between the observations in the ND and the FD is made using a simulation that convolves models of the neutrino flux, neutrino interactions, nuclear effects, and detector response. This gives rise to a host of complicating effects that muddy the simple picture. These complications come from two main sources. First, the identification efficiency is not 100 %, and there are some background events (for example, NC interactions with a π^0 present a background to ν_e CC interactions). Both the efficiency and background are imperfectly known. Because the background level tends to be similar in both the FD and ND, it helps if the ND can characterize backgrounds better than the FD.

The second aspect that complicates the simple picture is that the FD (and the similar ND) must use a target material composed of heavy nuclei. The target nucleus affects neutrino interactions in ways that ultimately drive the design of the ND complex. In particular, in heavy nuclei, the nucleons interact with each other and exhibit Fermi motion, providing moving targets for neutrino interactions. The wavelength of an interaction depends on momentum transfer but is often long enough to simultaneously probe multiple nucleons.

Another complication is that neutrino-nucleus scattering models rely on neutrino-nucleus cross sections, but neutrino cross sections on *free nucleons* are not generally well known in the kinematic range of interest to DUNE. Since the ND will enable high-statistics measurements on liquid and gaseous argon, rather than another nucleus, it will reduce nuclear model dependence. A final complication comes about because neutrinos produce hadrons within the nucleus. After production the hadrons undergo final-state interactions (FSI) and are thereby attenuated as they leave the target nucleus. Section **??** of Appendix **??** discusses neutrino-nucleus scattering in more detail.

Neutrons can be produced from the struck nucleus, as well as from follow-on interactions of the neutrino's reaction-products with other nuclei. The energy carried away by neutrons is difficult to detect and can bias the reconstructed neutrino energy. The SAND and MPD detectors have capabilities that allow neutron energy to be directly measured. The DUNE-PRISM program constrains the true-to-reconstructed energy relation and is thus also sensitive to energy carried by neutrons.

Heavy nuclei in the detector offer additional complications for particles that have left the struck nucleus, especially in the case where the detector is dense, e.g., in ArgonCube. Particles produced in a neutrino interaction may reinteract inside the detector, creating electromagnetic and hadronic cascades. These cascades, particularly the hadronic ones, confuse the reconstruction program due to overlapping energy and event features. They also cause a degradation of the energy resolution and result in additional energy carried by neutrons that may go missing. Particle identification by dE/dx is less effective for early showering particles, and low-energy particle tracks in a dense detector may be too short to detect. The HPgTPC in the MPD allows us to measure neutrino interactions on argon, but with significantly fewer secondary interactions and much lower-energy tracking thresholds.

Finally, setting aside complications due to heavy nuclei and dense detectors, we note that a significant fraction of the neutrino interactions in DUNE will come from inelastic processes, not the

simpler quasi-elastic (QE) scattering. This typically leads to a more complex morphology for events and greater challenges for the detector and the modeling. The DUNE ND acts as a control for the FD and is designed to be more capable than the FD at measuring complicated inelastic events.

These complexities are incorporated imperfectly into the neutrino interaction model. The predicted signal in the ND is a convolution of this interaction model with the beam model and the detector response model. The critical role of the ND is to supply the observations used to tune, or calibrate, this convolved model, thereby reducing the overall uncertainty in the expected signal at the FD, which is used for extracting the oscillation parameters via comparison with the observed signal. And with its high statistics and very capable subsystems, the ND will produce data sets that will provide the raw material for improving the models beyond simple tuning.

1.3 ND Hall and Construction

Figure 1.7 shows the current design of the underground hall required for the ND construction concept. The hall must house the detector components and enable the required off-axis movement. The layout shows the spaces required for the detector itself, and for safety and egress. This work is in progress.

The overall construction method means the conventional facilities (CF) must provide a primary access shaft that is large enough for lowering the pressure vessel and the magnet coils. In the figure, ArgonCube is shown in its on-axis construction position, as is the MPD. Because SAND does not move, it is placed in a dedicated alcove downstream of the other detectors.

The DUNE-PRISM design requires that both the MPD and ArgonCube be able to move horizontally to a position off the beam axis. The direction of the motion is to one side of the beam, with a maximum displacement of approximately 30.5 m.

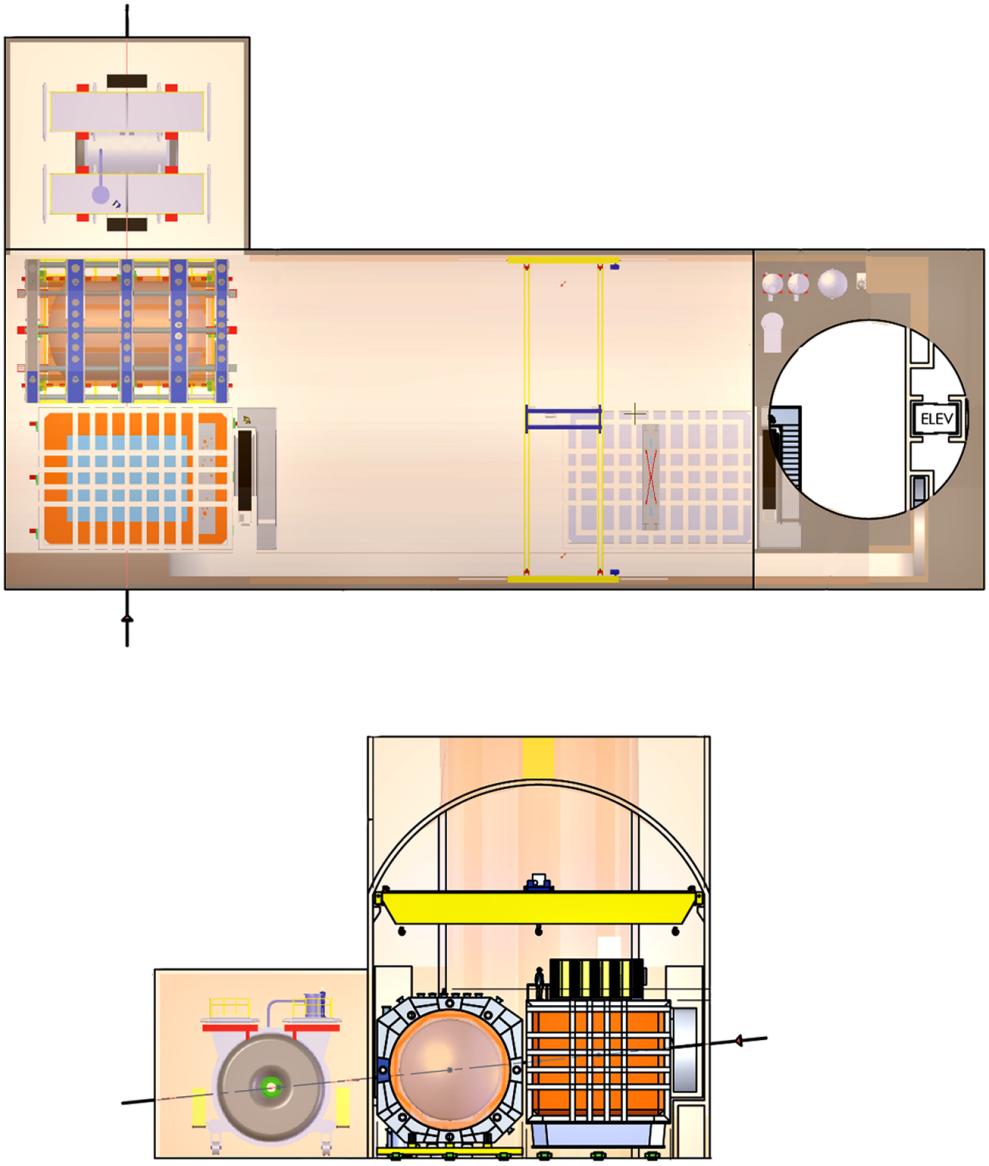


Figure 1.7: DUNE ND hall shown from above (top) and from the side transverse to the beam (bottom). The ArgonCube, MPD, and SAND are shown (in that order, bottom to top, in the upper figure) in position on the beam axis (black arrow) in both drawings.

Glossary

3D scintillator tracker (3DST) The core part of the 3D projection scintillator tracker spectrometer in the near detector conceptual design. 7, 10

ArgonCube The name of the core part of the Deep Underground Neutrino Experiment (DUNE) near detector (ND), a liquid argon time-projection chamber (LArTPC). 5, 8, 11–13

charged current (CC) Refers to an interaction between elementary particles where a charged weak force carrier (W^+ or W^-) is exchanged. 3, 8, 11

conventional facilities (CF) Pertaining to construction and operation of buildings and conventional infrastructure, and for LBNF and DUNE project (LBNF/DUNE), CF includes the excavation caverns. 12

charge parity (CP) Product of charge and parity transformations. 3

charge-parity symmetry violation (CPV) Lack of symmetry in a system before and after charge and parity transformations are applied. For CP symmetry to hold, a particle turns into its corresponding antiparticle under a charge transformation, and a parity transformation inverts its space coordinates, i.e., produces the mirror image. 2

Deep Underground Neutrino Experiment (DUNE) A leading-edge, international experiment for neutrino science and proton decay studies. 2–4, 6, 7, 11–13

DUNE Precision Reaction-Independent Spectrum Measurement (DUNE-PRISM) a mobile near detector that can perform measurements over a range of angles off-axis from the neutrino beam direction in order to sample many different neutrino energy distributions. 6, 11, 12

electromagnetic calorimeter (ECAL) A detector component that measures energy deposition of traversing particles (in the near detector conceptual design). 6, 7, 10

far detector (FD) The 70 kt total (40 kt fiducial) mass LArTPC DUNE detector, composed of four 17.5 kt total (10 kt fiducial) mass modules, to be installed at the far site at SURF in Lead, SD, USA. 2, 3, 5, 7–9, 11, 12

final-state interactions (FSI) Refers to interactions between elementary or composite particles subsequent to the initial, fundamental particle interaction, such as may occur as the products exit a nucleus. 11

high-pressure gaseous argon TPC (HPgTPC) A time projection chamber (TPC) filled with gaseous argon; a possible component of the DUNE ND. 6, 11

KLOE KLOE is a e^+e^- collider detector spectrometer operated at DAFNE, the ϕ-meson factory at Frascati, Rome. In DUNE it will consist of a 26 cm Pb+scintillating fiber ECAL surrounding a cylindrical open detector region that is 4.00 m in diameter and 4.30 m long. The ECAL and detector region are embedded in a 0.6 T magnetic field created by a 4.86 m diameter superconducting coil and a 475 tonne iron yoke. 7, 10

L/E length-to-energy ratio. 8

liquid argon (LAr) Argon in its liquid phase; it is a cryogenic liquid with a boiling point of −90 °C (87 K) and density of 1.4 g/ml. 5–7

liquid argon time-projection chamber (LArTPC) A TPC filled with liquid argon; the basis for the DUNE far detector (FD) modules. 4–7

Monte Carlo (MC) Refers to a method of numerical integration that entails the statistical sampling of the integrand function. Forms the basis for some types of detector and physics simulations. 9

multi-purpose detector (MPD) A component of the near detector conceptual design; it is a magnetized system consisting of a high-pressure gaseous argon TPC (HPgTPC) and a surrounding electromagnetic calorimeter (ECAL). 6, 11–13

neutral current (NC) Refers to an interaction between elementary particles where a neutrally charged weak force carrier (Z^0) is exchanged. 8, 11

near detector (ND) Refers to the detector(s) installed close to the neutrino source at Fermilab. 2–8, 11–13

PCB printed circuit board. 7

quasi-elastic (QE) Refers to interaction between elementary particles and a nucleus in an energy range where the interaction can be modeled as occurring between constituent quarks of one nucleon and resulting in no bulk recoil of the resulting nucleus. 12

System for on-Axis Neutrino Detection (SAND) The beam monitor component of the near detector that remains on-axis at all times and serves as a dedicated neutrino spectrum monitor. 7, 8, 11–13

silicon photomultiplier (SiPM) A solid-state avalanche photodiode sensitive to single photoelectron signals. 7

time projection chamber (TPC) A type of particle detector that uses an E field together with a sensitive volume of gas or liquid, e.g., liquid argon (LAr), to perform a 3D reconstruction of a particle trajectory or interaction. The activity is recorded by digitizing the waveforms of current induced on the anode as the distribution of ionization charge passes by or is collected on the electrode. 5–7, 10

References

[1] A. Friedland and S. W. Li, "Understanding the energy resolution of liquid argon neutrino detectors," *Phys. Rev.* **D99** no. 3, (2019) 036009, arXiv:1811.06159 [hep-ph].